



NRC Publications Archive Archives des publications du CNRC

Adipose-derived stem cells from both visceral and subcutaneous fat deposits significantly improve contractile function of infarcted rat hearts

Chi, Chao; Wang, Fei; Xiang, Bo; Deng, Jixian; Liu, Shangdian; Lin, Hung-yu; Natarajan, Kanmani; Li, Gang; Wang, Lei; Wang, Jian; Lin, Francis; Freed, Darren H.; Arora, Rakesh C.; Liu, Hongyu; Tian, Ganghong

This publication could be one of several versions: author's original, accepted manuscript or the publisher's version. / La version de cette publication peut être l'une des suivantes : la version prépublication de l'auteur, la version acceptée du manuscrit ou la version de l'éditeur.

For the publisher's version, please access the DOI link below. / Pour consulter la version de l'éditeur, utilisez le lien DOI ci-dessous.

Publisher's version / Version de l'éditeur:

<https://doi.org/10.3727/096368914X685780>

Cell Transplantation, 24, 11, pp. 2337-2351, 2015-11-11

NRC Publications Record / Notice d'Archives des publications de CNRC:

<https://nrc-publications.canada.ca/eng/view/object/?id=8568dede-6e82-40e6-98cb-79bb7c966e12>;

<https://publications-cnrc.canada.ca/fra/voir/objet/?id=8568dede-6e82-40e6-98cb-79bb7c966e12>

Access and use of this website and the material on it are subject to the Terms and Conditions set forth at

<https://nrc-publications.canada.ca/eng/copyright>

READ THESE TERMS AND CONDITIONS CAREFULLY BEFORE USING THIS WEBSITE.

L'accès à ce site Web et l'utilisation de son contenu sont assujettis aux conditions présentées dans le site

<https://publications-cnrc.canada.ca/fra/droits>

LISEZ CES CONDITIONS ATTENTIVEMENT AVANT D'UTILISER CE SITE WEB.

Questions? Contact the NRC Publications Archive team at

PublicationsArchive-ArchivesPublications@nrc-cnrc.gc.ca. If you wish to email the authors directly, please see the first page of the publication for their contact information.

Vous avez des questions? Nous pouvons vous aider. Pour communiquer directement avec un auteur, consultez la première page de la revue dans laquelle son article a été publié afin de trouver ses coordonnées. Si vous n'arrivez pas à les repérer, communiquez avec nous à PublicationsArchive-ArchivesPublications@nrc-cnrc.gc.ca.



Adipose-Derived Stem Cells From Both Visceral and Subcutaneous Fat Deposits Significantly Improve Contractile Function of Infarcted Rat Hearts

Chao Chi,^{*†‡} Fei Wang,^{*†‡} Bo Xiang,[‡] Jixian Deng,^{†‡} Shangdian Liu,^{*} Hung-Yu Lin,[†] Kanmani Natarajan,[§] Gang Li,^{*} Lei Wang,^{*} Jian Wang,[§] Francis Lin,[¶] Darren H. Freed,[#] Rakesh C. Arora,^{**} Hongyu Liu,^{*} and Ganghong Tian^{†‡}

^{*}Department of Cardiac Surgery, First Affiliated Hospital, Harbin Medical University, Harbin, China

[†]National Research Council, Winnipeg, Manitoba, Canada

[‡]Department of Physiology and Pathophysiology, Faculty of Medicine, University of Manitoba, Winnipeg, Manitoba, Canada

[§]Department of Vascular Surgery, Union Hospital, Tongji Medical College,

Huazhong University of Science and Technology, Hubei, China

[¶]Department of Physics and Astronomy, University of Manitoba, Winnipeg, Manitoba, Canada

[#]University of Alberta, Edmonton, Canada

^{**}St. Boniface Research Centre, Winnipeg, Manitoba, Canada

Adipose-derived stem cells (ASCs) from subcutaneous and visceral adipose tissues have been studied individually. No studies have compared their abilities in treatment of heart failure. This study was designed to evaluate whether ASCs from the two sources could provide a long-term improvement of cardiac function in infarcted hearts. Rat subcutaneous and visceral adipose tissues were excised for isolation of ASCs. Morphology, yield, proliferation, surface markers, differentiation, and cytokine secretion of the subcutaneous ASCs (S-ASCs) and visceral ASCs (V-ASCs) were analyzed. Then a rat model of myocardial infarction (MI) was established by a coronary occlusion. Seven days after occlusion, S-ASCs ($n=22$), V-ASCs ($n=22$), and Dulbecco's modified Eagle medium (DMEM, $n=20$) were injected into the infarct rim, respectively. Cardiac function was then monitored with MRI for up to 6 months. The hearts were then removed for histological assessments. The yield of V-ASCs per gram of the visceral adipose depot was significantly greater than that of S-ASCs in 1 g of the subcutaneous adipose depot. On the other hand, the S-ASCs showed a greater proliferation rate and colony-forming unit relative to the V-ASCs. In addition, the infarcted hearts treated with either S-ASCs or V-ASCs showed a significantly greater left ventricular ejection fraction (LVEF) than those treated with DMEM at 4 weeks and 6 months following the cell/DMEM transplantation. Moreover, the infarct sizes of both S-ASC- and V-ASC-treated hearts were significantly smaller than that in the DMEM-treated hearts. MRI showed the implanted ASCs at the end of 6 months of recovery. Despite the differences in cell yield, proliferation, and colony formation capacity, both S-ASCs and V-ASCs provide a long-lasting improvement of cardiac contractile function in infarcted hearts. We conclude that the subcutaneous and visceral adipose tissues are equally effective cell sources for cell therapy of heart failure.

Key words: Subcutaneous adipose-derived stem cells; Visceral adipose-derived stem cells; Myocardial infarction; Heart failure; Magnetic resonance imaging

INTRODUCTION

Cardiovascular disease is a leading cause of morbidity and mortality in developed countries, and its prevalence in developing countries has risen rapidly in recent years. Myocardial infarction (MI) plays an important role in this setting. MI results in a significant loss of the cardiomyocytes, leading to cardiac dysfunction and heart failure.

It is well known that the adult cardiomyocytes have a very limited capacity of self-renewal. Therefore, exogenous regenerative strategies need to be developed to revitalize the injured myocardium and resume normal cardiac function. A number of studies have suggested that stem cells may hold great promise for rebuilding of a healthy heart and prevention of heart failure (6,23,28).

Received July 11, 2014; final acceptance December 16, 2014. Online prepub date: January 5, 2015.

[†]These authors provided equal contribution to this work.

Address correspondence to Dr. Hongyu Liu, Department of Cardiac Surgery, First Affiliated Hospital, Harbin Medical University, 23 Youzheng St, Nangang, Harbin, Heilongjiang 150001, China. Tel: +8645185555817; Fax: +8645185555817; E-mail: hylu1963@gmail.com or Dr. Ganghong Tian, National Research Council Canada, 435 Ellice Ave, Winnipeg, Manitoba, Canada R3B, 1Y6. Tel: +1 (204) 984-6654; Fax: +1 (204) 984-7036; E-mail: hong.tian@nrc-cnrc.gc.ca

Our previous study has shown that intramyocardial injection of the adipose-derived stem cells (ASCs) extracted from the subcutaneous fat tissue significantly reduced infarct size and improved contractile function of infarcted rat hearts (35). On heart tissue sections, we found that the implanted subcutaneous ASCs (S-ASCs) expressed cardiomyocyte contractile fibril-specific proteins 1 month after the cell transplantation (35). Moreover, it was found that coculture of the S-ASCs with the neonatal cardiomyocytes induced cardiomyogenic differentiation of the stem cells (35). Other investigators reported similar findings (4,31). In addition, a sufficient amount of subcutaneous adipose tissue can be readily harvested with a minimally invasive procedure. These studies suggest that subcutaneous adipose tissue could be a stem cell source for use in the treatment of MI and heart failure (3,36). Recently, visceral adipose tissue has gradually gained a great deal of attention as to its physiological function and biological properties, particularly with respect to its differences from subcutaneous adipose tissue (13). It has been shown that visceral adipose tissue differs significantly from subcutaneous adipose tissue in energy storage, endocrine function, lipolytic activity, and response to insulin (15,17). In 2009, Baglioni and colleagues successfully isolated a population of adult stem cells from the omental adipose tissue of human patients (2). Subsequently, several studies showed that visceral ASCs (V-ASCs) had different profiles in gene expression, adiponectin release, and insulin signaling in comparison with S-ASCs (25). Thus, the cardioprotective effects exhibited by S-ASCs should not be simply extrapolated to V-ASCs. Only limited studies have assessed cardioprotective effects of V-ASCs (10,18). Therefore, this study was designed to comparatively analyze cardioprotective effects of S-ASCs and V-ASCs. Moreover, most studies only evaluated short-term (1 to 2 months) cardioprotective function of ASCs. Thus, it is uncertain whether transplantation of ASCs provides long-lasting cardiac function improvement. To answer this question, we monitored cardiac function for 6 months after cell transplantation in this study.

MATERIALS AND METHODS

The animals used in this study received humane care in compliance with the *Guide to the Care and Use of Experimental Animals* formulated by the Canadian Council on Animal Care. The Animal Care Committee of the National Research Council Canada and Harbin Medical University approved the experimental protocols of this study.

In total, 108 inbred Lewis rats (Charles River Laboratories, Sherbrooke, QC, Canada) were used in this study. Among them, 98 female rats were used for establishment of myocardial infarction, and 10 male rats were used for harvesting adipose tissue. Fourteen rats died after the surgery of coronary occlusion. Twenty rats died after

the surgery for intramyocardial injection of stem cells or Dulbecco's modified Eagle medium (DMEM; HyClone, Logan, UT, USA).

Preparation of ASCs

Ten male inbred Lewis rats were humanely euthanized for collection of the adipose tissues. Subcutaneous adipose tissue was obtained from the inguinal fat deposit. Visceral adipose tissue was taken from mesenteric, epididymal, and perirenal fat deposits. To minimize individual variability, the two types of adipose tissues were harvested from all the animals. ASCs were then isolated from the adipose tissues according to the method developed by Zuk and colleagues (38) with some modifications. In brief, the excised adipose tissue was washed extensively with phosphate-buffered saline (PBS; HyClone) to remove contaminating debris and blood cells. The adipose tissue was minced and digested with collagenase I (2 mg/ml; Worthington Biochemical, Lakewood, NJ, USA) at 37°C for 20–30 min. Collagenase activity was then neutralized by changing the enzyme medium with a complete medium. The complete medium contains DMEM with 15% fetal bovine serum (FBS; HyClone), 50 µg/ml streptomycin (HyClone), and 50 IU/ml penicillin (HyClone). The digested adipose tissue was filtered with a 100-µm and then with a 25-µm nylon membrane (BD Falcon, Bedford, MA, USA) to eliminate the undigested fragments. The cellular suspension was centrifuged at 300×g for 10 min. The cell pellets were resuspended in the complete medium and cultivated for 48 h at 37°C in 5% CO₂. The cells that did not attach to the plastic surface were removed. The adherent cells were disassociated with 0.25% trypsin (Life Technologies, Burlington, ON, Canada) and counted with an automated cell counter (Countess; Life Technologies). The adherent cells were collected for subsequent *in vitro* and *in vivo* studies.

In order to render them visible on magnetic resonance imaging (MRI), ASCs were incubated for 2 days in the complete medium containing 25 µg/ml superparamagnetic iron oxide (SPIO) nanoparticles (Feridex; Bayer HealthCare, Whippany, NJ, USA) and 1 µg/ml polylysine (PLL; Sigma-Aldrich, St. Louis, MO, USA). The latter was used as a transfecting agent. For identifying the implanted cells on the tissue section, the ASCs were transfected with a lentiviral vector encoding a gene for emerald green fluorescent protein (GFP). The transfection process was described in our previous study (35).

Fluorescence-Activated Cell Sorting (FACS)

Characteristic surface markers (cluster of differentiation, CD) of the S-ASCs and V-ASCs from three animals were determined using flow cytometry (FACSCalibur; BD Biosciences, Mississauga, ON, Canada). Briefly, 10⁶ live cells at the third to fifth passages were suspended in 100 µl wash flow buffer (WFB). The WFB contains

1× PBS, 2% FBS, 0.05% sodium azide (Sigma-Aldrich). Then the ASCs were incubated with antibodies of interest at 4°C for 30 min. The antibodies used in this study included CD11b-Alexa Fluor 488 (1:200 dilution, 201812; Biolegend, San Diego, CA, USA), CD29-Alexa Fluor 488 (1:50 dilution, 102212; Biolegend), CD31-Alexa Fluor 488 (1:10 dilution, MCA1334A488; AbD Serotec, Raleigh, NC, USA), CD45-phycoerythrin (PE) (1:100 dilution, 202207; Biolegend), CD59-fluorescein isothiocyanate (FITC) (1:20 dilution, 550976; BD Biosciences), CD90-FITC (1:200 dilution, 202504; Biolegend), and CD106-PE (1:20 dilution, 200403; Biolegend). For assessment of CD73 expression, the ASCs were incubated with primary antibody CD73 (1:50 dilution, 551123; BD Biosciences) at 4°C for 30 min and then washed with PBS three times and stained with second antibody goat anti-mouse IgG-FITC (1:100 dilution, sc-2010; Santa Cruz Biotechnology, Santa Cruz, CA, USA) at 4°C for 1 h. FACS was performed using 20,000 cells per sample.

Colony-Forming Unit Assay

One of the prominent properties of multipotent stem cells is their ability to generate discrete cell clusters or colonies. To assess their colony-forming capacity, approximately 100 S-ASCs and 100 V-ASCs were plated in individual 10-cm dishes (BD Falcon). After 14 days of cultivation in the complete medium, the ASCs were fixed, dehydrated, and stained with 10% formalin (VWR International, West Chester, PA, USA), 90% ethanol (Commercial Alcohols Inc., Brampton, ON, Canada), and 0.5% Eosin Y solution (Sigma-Aldrich), respectively. The frequency of colony-forming units was then determined by counting individual colonies. Only the cell clusters with a diameter greater than 1 mm were counted.

Assessment of ASC Proliferation

Proliferation potentials of S-ASCs and V-ASCs were assessed by measuring their cumulative population doubling level (CPDL) (29). S-ASCs and V-ASCs were plated on individual 10-cm dishes at a density of 10^5 cells/dish. After 3 days of cultivation in the complete medium, the ASCs were collected, counted, and replated on fresh 10-cm dishes at the same density. This process (plating, cultivating, and collecting) was repeated seven times. The population doubling (PD) level at each passage was calculated using the equation: $PD = \ln(N_f/N_i)/\ln 2$, where N_i and N_f are initial and final cell numbers, respectively, and \ln is the natural log. The PDs of the consecutive subcultures were added to yield their CPDL.

Adipogenic and Osteogenic Inductions

Adipogenic induction was induced by incubation of the cells for 8 days in a medium containing DMEM, 10% FBS, 10 μ M insulin (Sigma-Aldrich), 0.5 mM isobutyl-

methylxanthine (Sigma-Aldrich), 200 μ M indomethacin (Sigma-Aldrich), 1 μ M dexamethasone (Sigma-Aldrich), 5 μ g/ml streptomycin, and 5 U/ml penicillin. Osteogenic induction was carried out by cultivating the cells for 21 days in a culture medium containing DMEM, 10% FBS, 10 mM β -glycerophosphate (Sigma-Aldrich), 50 μ M ascorbate-2-phosphate (Sigma-Aldrich), 10 nM 1,25-(OH)₂ vitamin D₃ (Sigma-Aldrich), 50 μ g/ml streptomycin (HyClone), and 50 IU/ml penicillin (HyClone).

Adipogenic differentiation of the ASCs was determined by staining intracellular lipid deposits and assessing the gene expressions of lipoprotein lipase (LPL) and peroxisome proliferator-activated receptor- γ (PPAR- γ). Osteogenic differentiation was evaluated by staining intracellular alkaline phosphatase (AP) and monitoring of the expression of SPP1 (secreted phosphoprotein 1) and Sp7 (Sp7 transcription factor). ASCs cultured in the complete medium were used as a control. Each of the induction assays was conducted three times.

To determine differentiation percentages of S-ASCs and V-ASCs, the two types of the ASCs were plated onto individual 10-cm dishes at a density of 100 cells/dish and cultured in complete medium. Once colonies were established, adipogenic and osteogenic induction were initiated at the individual dishes. At end of the inductions, the cell colonies were stained with Oil red O (Sigma-Aldrich) and Alkaline Phosphatase kit (Sigma-Aldrich). The unstained colonies were verified with 0.5% Eosin Y. The percentages of the colonies stained positive for Oil red O or alkaline phosphatase were then determined to estimate the differentiation potential of both ASCs.

Immunocytology

To analyze the ASC cytokine expression, ASCs were cultured on the coverslips (VWR International) until confluence. The ASCs were then fixed with 4% paraformaldehyde (Alfa Aesar, Ward Hill, MA, USA) in PBS for 1 h, and treated with 0.1% Triton X-100 (Sigma-Aldrich) for 15 min. After blocking with 3% bovine serum albumin (BSA, Sigma-Aldrich) in PBS at room temperature for 1 h, the slides were incubated with rabbit polyclonal anti-vascular endothelial growth factor (VEGF) antibody (1:100 dilution, sc-507; Santa Cruz Biotechnology), goat polyclonal anti-insulin-like growth factor-1 (IGF-1) antibody (1:100 dilution, sc-1422; Santa Cruz Biotechnology), or rabbit polyclonal anti-hepatocyte growth factor (HGF) antibody (1:100 dilution, sc-7949; Santa Cruz Biotechnology) at 4°C overnight. After incubation with secondary antibody Alexa Fluor 594 goat anti-rabbit IgG antibody (1:200 dilution, A11012; Life Technologies) or Alexa Fluor 594 donkey anti-goat IgG antibody (1:200 dilution, A11058; Life Technologies) at room temperature for 1 h, cell nuclei were counterstained with 4',6-diamidino-2-phenylindole dihydrochloride (DAPI; Santa Cruz Biotechnology).

The images were taken with a fluorescence microscope (Zesis Axio observer Z1 Inverted microscope; Carl Zesis Canada Ltd., Toronto, ON, Canada).

RT-PCR

Reverse-transcription polymerase chain reaction (RT-PCR) was performed to determine expressions of VEGF, HGF, IGF-1, LPL, PPAR- γ , SPP1, and Sp7 by the ASCs. mRNA was extracted from both S-ASCs and V-ASCs using an RNA extraction kit (Qiagen, Mississauga, ON, Canada). One microgram of mRNA was reversely transcribed using SuperScript III reverse transcriptase (Life Biotechnologies). The sequences of all the primers used in this study are detailed in Table 1.

Animal Model and Experimental Protocol

Inbred female Lewis rats with an average body weight of 200 g underwent an open-chest surgery for a permanent occlusion of the left anterior descending coronary artery (LAD) to establish a model of MI and heart failure. The surgery was performed under an inhalational anesthesia with isoflurane (Baxter Corporation, Mississauga, ON, Canada). Respiration was controlled with a rodent ventilator (Columbus Instruments, Columbus, OH, USA) at a rate of 60–70 breaths/min and tidal volume of 2 to 3 ml. A left anterior thoracotomy was made through the fourth intercostal space. The LAD was permanently occluded at ~2 mm from its origin using a 6-0 silk suture (Ethicon, Somerville, NJ, USA). The chest was then closed.

One week after LAD occlusion, the animals were randomly divided into six groups. The animals' chests were reopened under the same anesthesia described above. In groups I ($n=11$) and IV ($n=11$), four injections of $\sim 1.25 \times 10^6$ GFP/SPIO-labeled S-ASCs with total volume of 40 μ l were made into infarct rim using a 30-gauge needle. Rats in groups II ($n=11$) and V ($n=11$) received four intramyocardial injections of GFP/SPIO-labeled V-ASCs at the same dosage. Animals in groups III ($n=10$) and VI ($n=10$) received intramyocardial injections of DMEM and were used as a control. After the injections, animals in groups I, II, and III were allowed to recover for 1 month, whereas those in groups IV, V, and VI recovered for 6 months. During the recovery, cardiac function and the implanted cells were monitored twice using MRI. At end of the recovery periods, animals were euthanized. Animal hearts were removed and sectioned into 8- μ m tissue slices for histological analysis. It should be mentioned that only animals that survived the entire protocol were included in the sample sizes of the six groups.

Iron Staining, Immunohistological and Histological Analysis

SPIO on the tissue slices were detected using the Prussian blue staining method. Briefly, the tissue slices were incubated in a medium containing 2% potassium hexacyanoferrate (II)-trihydrate (Sigma-Aldrich) and 0.2 M hydrochloric acid (Fisher Scientific, Nepean, ON, Canada)

Table 1. Primers of Specific Markers for Differentiation and Cytokines

Gene	Primer Sequences	Fragment (bp)	GenBank No.
LPL	F, 5' AGCAAGGCATACAGGTGCAA 3' R, 5' GTCAGCCCGACTTCTTCAGAG 3'	571	NM_012598.2
PPAR- γ	F, 5' CTACACCATGCTGGCCTCCCTGATG 3' R, 5' TTGTCAGCGACTGGGACTTTTCTGC 3'	481	NM_013124
SPP1	F, 5' CCATGAGACTGGCAGTGGTTTGCT 3' R, 5' GACCTCAGTCCGTAAGCCAAGCTA 3'	463	NM_012881.2
Sp7	F, 5' GTAATCTTCGTGCCAGACCTCTTG 3' R, 5' GACACTAGGCAGGCAGTCAGAAG 3'	405	NM_001037632.1
VEGF	F, 5' TGGACCCTGGCTTTACTGCT 3' R, 5' AACCGGGATTTCTTGCGCTT 3'	449	NM_031836
HGF	F, 5' TCCCCTATGCAGAAGGACAGA 3' R, 5' AAAGCTGTGTTTCATGGGGGAT 3'	410	NM_017017.2
IGF-1	F, 5' CATGTCGTCTTCACATCTCTTCTAC 3' R, 5' CTTGTGTGTCGATAGGGGCTGGGAC 3'	349	NM_001082477
GAPDH	F, 5' ATCTGACATGCCGCTGGAGAAACC 3' R, 5' CAGGGTTTCTTACTCCTTGGAGGCC 3'	287	NM_017008

Notes: LPL, lipoprotein lipase; PPAR- γ , peroxisome proliferator-activated receptor gamma; SPP1, secreted phosphoprotein 1; Sp7, Sp7 transcription factor; VEGF, vascular endothelial growth factor; HGF, hepatocyte growth factor; IGF-1, insulin-like growth factor-1; GAPDH, glyceraldehyde-3-phosphate dehydrogenase; F, forward; R, reverse; bp, base pairs.

for 15 min. After the staining process, the tissue sections were examined under the Zeiss inverted microscope.

Two methods were used to detect the implanted GFP-labeled ASCs in tissue sections. The first method was simply monitoring of GFP expression on the tissue sections with the Zeiss microscope. The second method was immunostaining GFP first with GFP antibody. Briefly, the tissue sections were incubated overnight at 4°C in a 1% BSA media containing primary antibody (anti-GFP rabbit IgG, 1:100 dilution; Life Technologies). The sections were then rinsed three times with PBS, followed by 1-h incubation in a secondary antibody (Alexa-Fluor 594-conjugated goat anti-rabbit IgG, 1:200 dilution; Life Technologies). The stained sections were then examined with the same fluorescence microscope.

To assess myocardial infarction, heart tissue sections were stained with Masson trichrome (Polyscience Inc., Warrington, PA, USA) protocol. After Masson trichrome staining, the tissue sections were examined with a Leica microscope (Aperio CS2 microscope; Leica Microsystems Inc., ON, Canada). Myocardial infarction was quantified as a percentage of left ventricular transverse perimeter occupied by collagen.

Cardiac MRI

Cardiac MRI scans were performed to track the implanted ASCs and to assess their effects on cardiac function. Animals were placed in a prone position in a cradle. Standard limb leads were established with electrodes placed on both forepaws and the left hind paw. The cradle was then inserted into an in-house-built quadrature MR coil. The coil was positioned in the center of the horizontal bore of a 7-Tesla Bruker magnet interfaced to a Bruker Biospec console (Bruker, Karlsruhe, Germany). Cardiac MR imaging acquisitions were triggered by both respiratory and ECG signals.

Cardiac cine imaging was performed using a gradient-echo sequence with a repetition time of 9.2 ms, echo time of 3.5 ms, field of view of 8×8 cm², and matrix size of 256×256. The cine images were acquired from five consecutive slices along the cardiac short axis with a slice thickness of 2.0 mm without gaps. Depending on the subject's heart rate, 15–18 frames were typically fit into one cardiac cycle. With a signal averaging of four k-space lines in each image, the total acquisition time for the five-slice cine images was approximately 43 min.

Image Process and Data Analysis

Cine MR images were analyzed using the image processing software Marevisi (National Research Council Canada, Winnipeg, Canada). In a set of cine images, the image with the smallest chamber area was considered to represent the end systole (ES), whereas the image with the largest chamber area was considered to reflect end diastole

(ED). Left ventricular (LV) endocardial and epicardial contours were drawn semiautomatically on serial short-axis images to obtain LV area at ES (LVA_{ES}) and ED (LVA_{ED}). Manual adjustments were made when required. LV ejection fraction (LVEF) was estimated using the equation of $[\Sigma LVA_{ED} - \Sigma LVA_{ES}] / \Sigma LVA_{ED} \times 100\%$, where ΣLVA_{ED} and ΣLVA_{ES} are the sum of LV area in all slices measured at ED and ES, respectively. The average value of LVA_{ED} was estimated using equations $\Sigma LVA_{ED} / N$, where N is the total number of the MRI slice.

Statistical Analysis

Statistical analyses were performed using Statistica (Statsoft, Tulsa, OK, USA). Student's *t*-test was used to define significant differences between S-ASCs and V-ASCs in cell surface markers, plastic surface adherence, clone formation, Oil red O/AP staining, and cytokine expression (VEGF, IGF-1, and HGF). One-way analysis of variance (ANOVA) in conjunction with Tukey's HSD post hoc test was used to determine significant differences in differentiation markers between the induced and control ASCs. One-way ANOVA with Tukey's HSD post hoc test was also used to determine significant difference in LVEF, LVA_{ED}, and infarct size among the six groups of the hearts.

RESULTS

Both S-ASCs and V-ASCs exhibited typical fibroblast-like spindle morphology on culture dishes (Fig. 1). It was noted that the cells enlarged gradually as cell culture continued, which may be related to cell aging. In addition, both of them expressed comparable significant levels of CD29, CD59, CD73, and CD90 with negligible expressions of hematopoietic antigens, such as CD11b, CD31, CD45, and CD106 (Fig. 1). This suggests that the two types of ASCs share common biological properties, at least from morphological and phenotypic points of view.

In addition, we found that the visceral adipose tissue gave rise to significantly more plastic adherent cells (6.5×10^5 cells/g tissue) than the subcutaneous adipose tissue (1.8×10^5 cells/g tissue) after primary tissue digestion. If the adherent cells were considered as ASCs, the visceral adipose tissue had a significantly higher frequency of ASCs than did the subcutaneous adipose tissue. However, the number of the colonies derived from S-ASCs (13.5 ± 2.6 colonies/100 ASCs) was greater than that from V-ASCs (9.8 ± 1.0 colonies/100 ASCs) under our experimental conditions (Fig. 2), suggesting that the colony-forming capacity of the S-ASCs was greater than that of V-ASCs.

To assess their proliferation rate, the two types of the ASCs were cultured in the complete medium, and their CPDL were determined. In the first week of culturing, the S-ASCs and V-ASCs showed comparable CPDL (Fig. 2). From the second week, however, CPDL of the S-ASCs

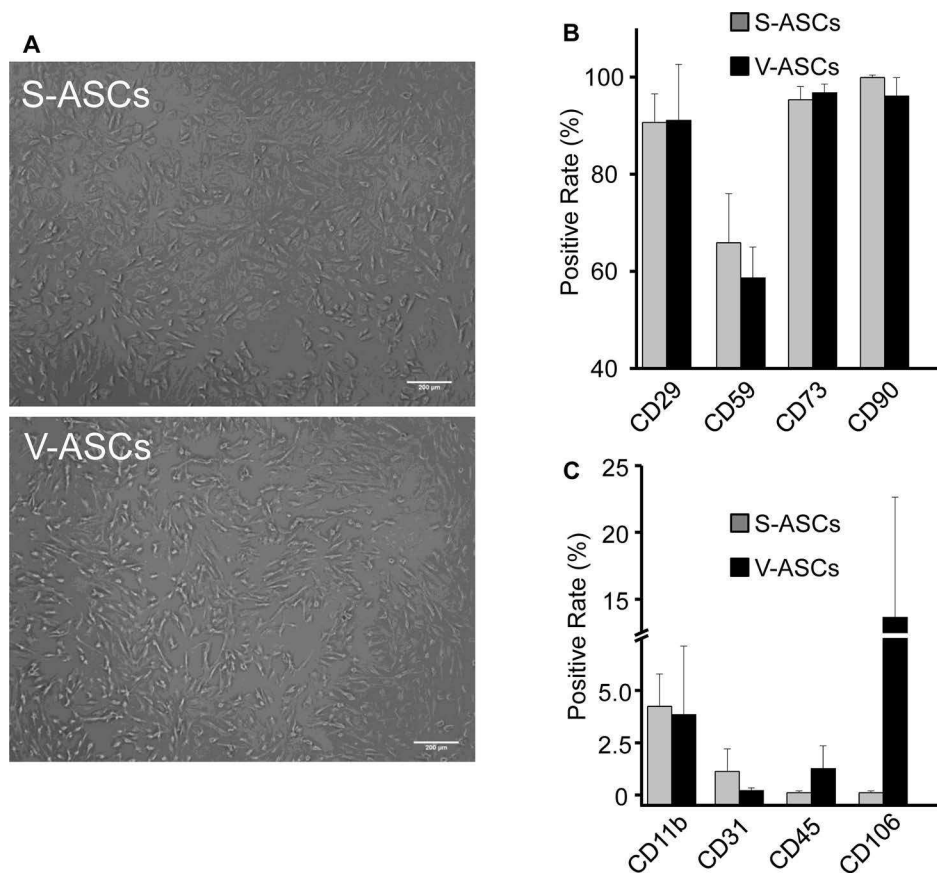


Figure 1. Representative morphology and cell-surface marker profile of subcutaneous adipose-derived stem cells (S-ASCs) and visceral adipose-derived stem cells (V-ASCs). Most ASCs from the two sources showed fibroblast-like morphology (A). In addition, both S-ASCs and V-ASCs expressed significant levels of CD29, CD59, CD73, and CD90 (B) with negligible expressions of CD11b, CD31, CD45, and CD106 (C). Expressions of the CD markers were not significantly different between S-ASCs ($n=3$) and V-ASCs ($n=3$). Scale bars: 200 μm .

became significantly greater than that of V-ASCs (Fig. 2). The difference in growth rate was also found between the two types of the human ASCs by other investigators (1).

Multidifferentiation potential is a key characteristic of mesenchymal stem cells (MSCs). To assess their differentiation capacity in this study, both ASCs were subjected to adipogenic and osteogenic inductions. After 8 days of adipogenic induction, approximately 67% of S-ASCs and 66% V-ASCs were stained positive for intracellular lipid droplets (Fig. 3). RT-PCR showed a significant increase in expression of the markers for adipogenic differentiation (LPL and PPAR- γ) in both ASCs (Fig. 4). Likewise, both ASCs were stained positive for alkaline phosphatase (Fig. 3) and expressed a similar level of osteogenic markers (SPP1 and Sp7), following 21 days of the induction.

Paracrine actions have been proposed as one of the fundamental mechanisms responsible for the observed therapeutic benefits of stem cells (9,22). VEGF, IGF-1, and HGF have all been shown to play important roles in angiogenesis and tissue remodeling. Thus, expression of

the cytokines in both ASCs was assessed in this study. It was found that the freshly isolated ASCs from the two sources were all stained positive for the three cytokines (Fig. 5). RT-PCR results further confirmed their intrinsic expressions of the cytokines (Fig. 5).

To assess short-term effects of the ASCs on cardiac contractile function, the rats in groups I, II, and III were allowed to recover for 4 weeks after transplantation of S-ASCs, V-ASCs, and DMEM, respectively. Cine MR imaging showed that LVEF of both S-ASC- and V-ASC-treated hearts were significantly higher than that of the DMEM-treated hearts at both 1 week and 4 weeks after the transplantations (Fig. 6). Differences in LVEF between the two ASC-treated groups were not statistically significant. Moreover, LVEFs measured at 1 and 4 weeks within each group were comparable.

The animals in groups IV, V, and VI were allowed to recover for 6 months for evaluation of the long-term effects of the ASCs on cardiac function. We found that LVEF at 1 month and 6 months of recovery was

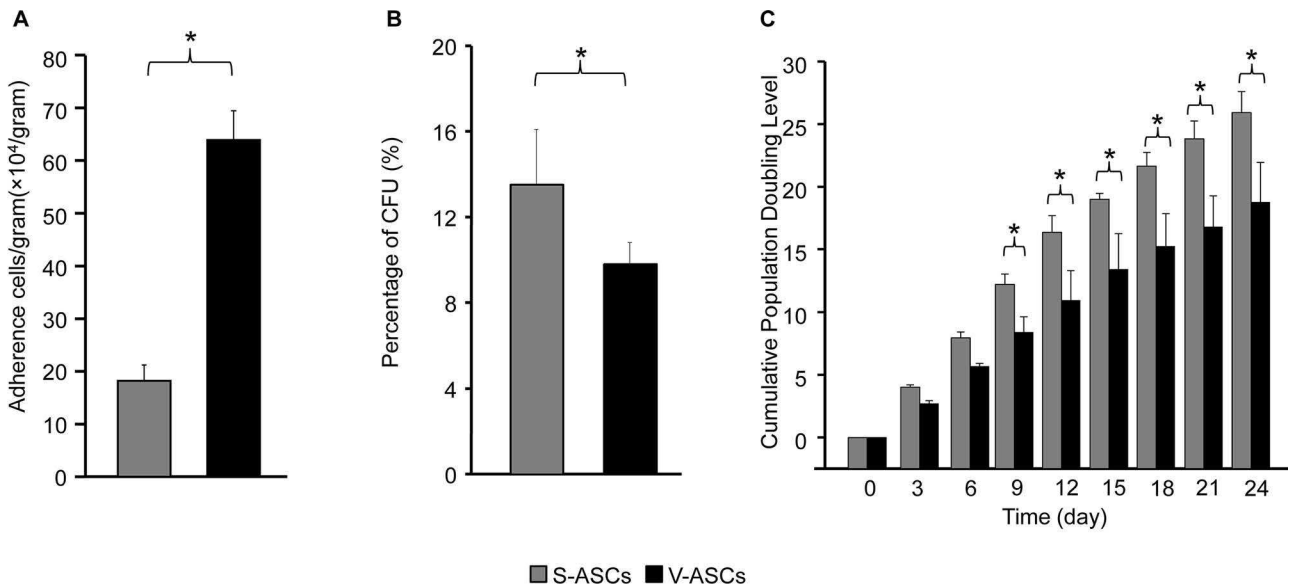


Figure 2. Basic biological properties of the S-ASCs and V-ASCs. Frequencies of adherent cells in 1 g of subcutaneous and visceral fat deposits (A), colony-forming unit percentage of the adherent cells from the two fat deposits (B), and cumulative population doubling level (CPDL) of subcutaneous adipose-derived stem cells (S-ASCs) and visceral adipose-derived stem cells (V-ASCs, C). It is clear that the visceral fat deposit contained significantly ($p < 0.05$, $n = 6$) more plastic adherent cells than the subcutaneous adipose deposit (A). However, colony-forming unit percentage of the visceral adherent cells was slightly but significantly ($p < 0.05$, $n = 6$) less than that of the subcutaneous adherent cells (B). The S-ASCs showed a significantly greater CPDL than V-ASCs did at the 9 days of culture and on (C, $n = 6$).

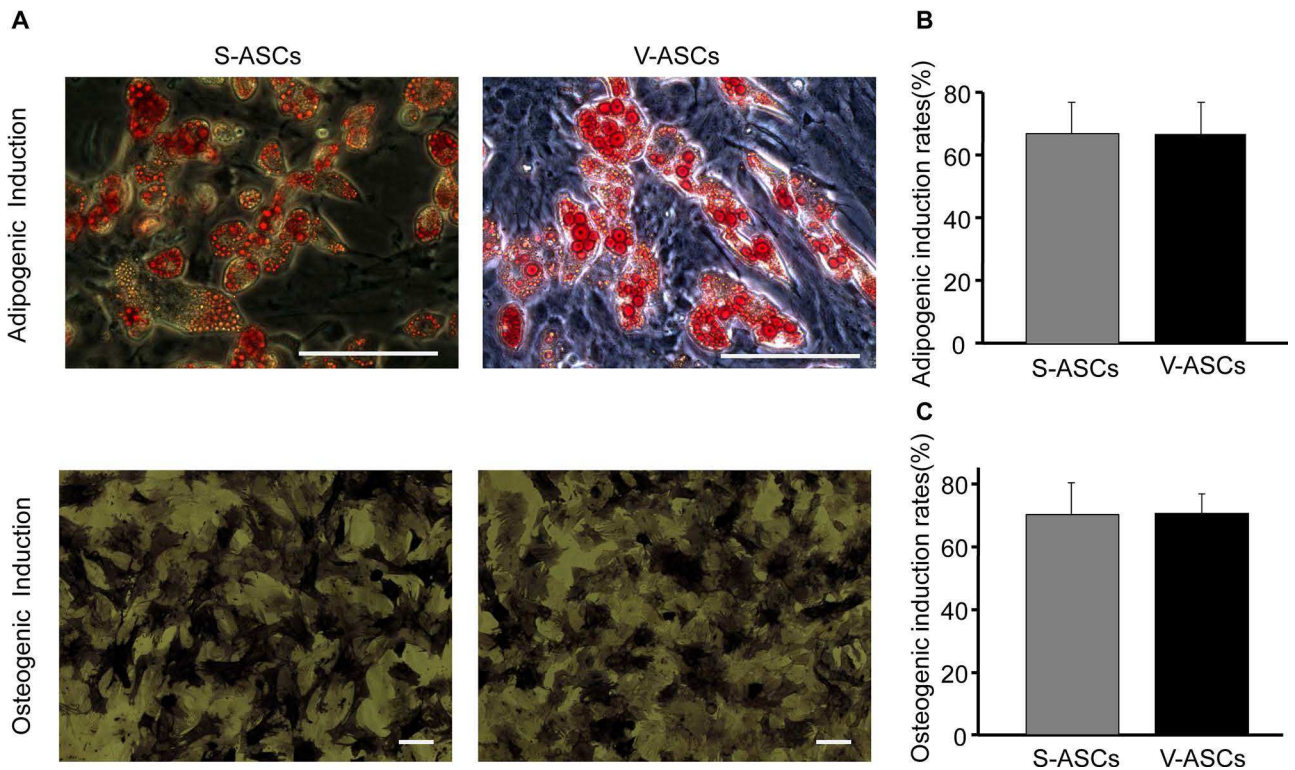


Figure 3. Histological assessment of adipogenic and osteogenic differentiations of the S-ASCs and V-ASCs. Pictures of Oil red O- and alkaline phosphatase (AP)-stained S-ASCs and V-ASCs after adipogenic and osteogenic inductions, respectively (A). The percentages of the colonies stained positive for Oil red O and AP were not significantly different between S-ASCs and V-ASCs (B and C, $n = 6$). Scale bars: 100 μ m.

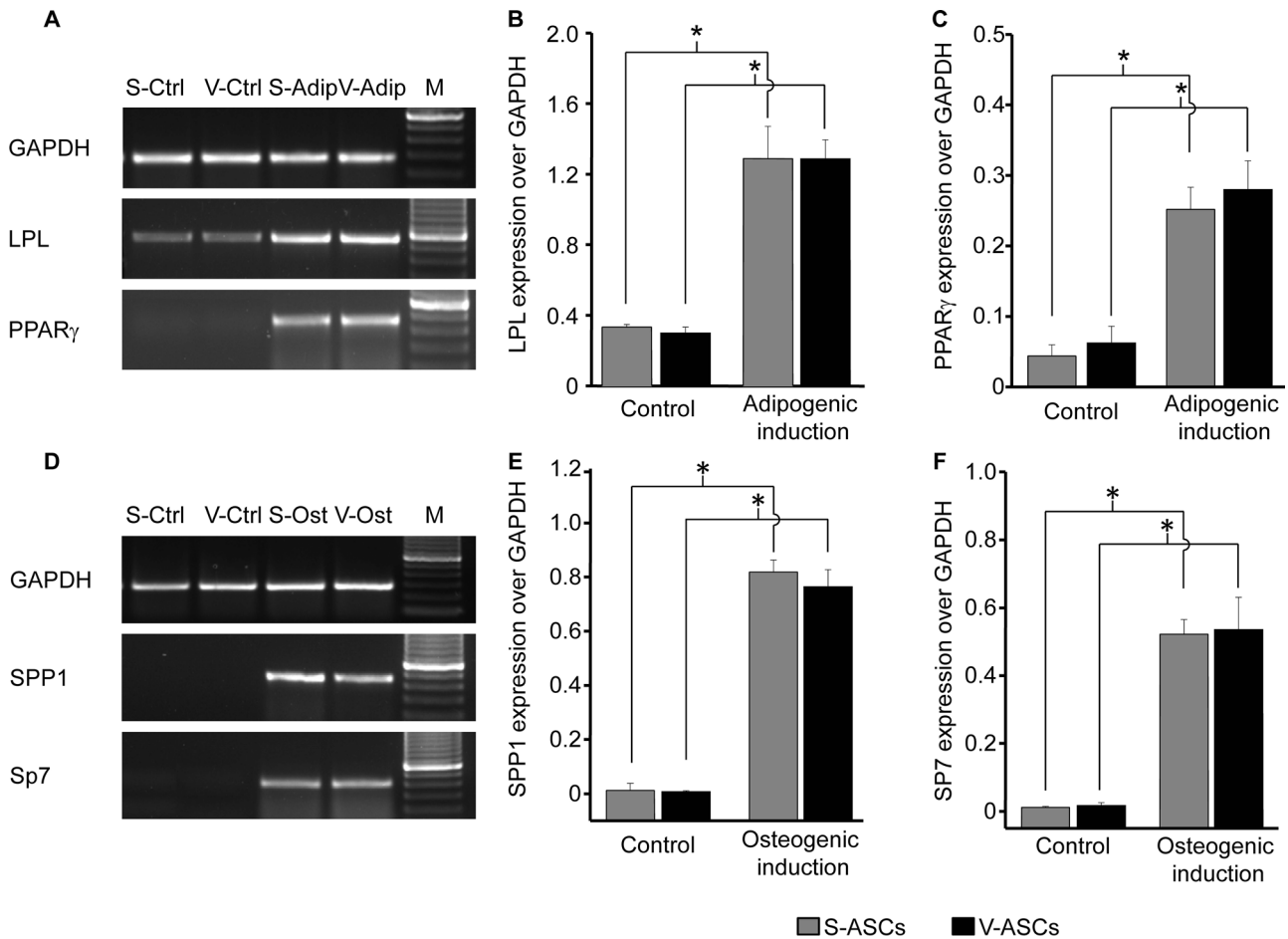


Figure 4. RT-PCR analysis of marker genes for adipogenic and osteogenic differentiation of S-ASCs and V-ASCs. LPL and PPAR- γ were detected in S-ASCs and V-ASCs subjected to adipogenic induction (A). The expressions of LPL and PPAR- γ were significantly greater in the induced S-ASCs and V-ASCs than in the control S-ASCs and V-ASCs (B and C, $n=3$). Expression of SPP1 and SP7 were detected in the S-ASCs and V-ASCs following osteogenic induction (D). The expressions of SPP1 and SP7 in the induced S-ASCs and V-ASCs were significantly higher than in the control S-ASCs and V-ASCs (E and F, $n=3$). The expressions of SPP1 and SP7 were not significantly different between the induced S-ASCs and V-ASCs. * $p<0.05$.

significantly greater in the S-ASC- and V-ASC-treated hearts than in the DMEM-treated hearts (Fig. 6). Again, LVEF between the two ASC-treated groups was not significantly different at the two time points. The results indicate that ASCs from both subcutaneous and visceral deposits provide comparable improvement on cardiac contractile function. Figure 6 also shows comparisons of LVA_{ED} of the rat hearts treated with S-ASCs or V-ASCs or DMEM at three time points of recovery. It was found that differences in LVA_{ED} among the three groups were not statistically significant at 1 week and 4 weeks of recovery (Fig. 6C). At 6 months of recovery, LVA_{ED} was significantly smaller in the ASC-treated hearts than in the DMEM-treated hearts (Fig. 6C), indicating that ASCs from the two sources could attenuate infarction-induced myocardial remodeling. However, it is clear that LVA_{ED} at 6 months was significantly greater than those at 1 and

4 weeks of recovery in all three groups (Fig. 6D), indicating that LV dilation did occur in all the three groups by 6 months of recovery, and ASCs could not completely prevent LV dilation.

As mentioned above, the rat hearts were removed from animals at the end of the recovery for assessment of myocardial infarction. No significant difference in infarct size was found between the S-ASC- and V-ASC-treated hearts ($p>0.05$) at 4 weeks or 6 months after transplantation. However, infarct sizes of the DMEM-treated hearts (groups III and VI) were significantly greater than those in the S-ASC- or V-ASC-treated hearts (groups I, II, IV, and V) (Fig. 7). This indicates that both S-ASCs and V-ASCs may prevent infarction-associated cardiomyocyte loss and enhance cardiac regeneration.

In addition, MR images acquired from the ASC-treated hearts at the end of 6 months of recovery clearly show

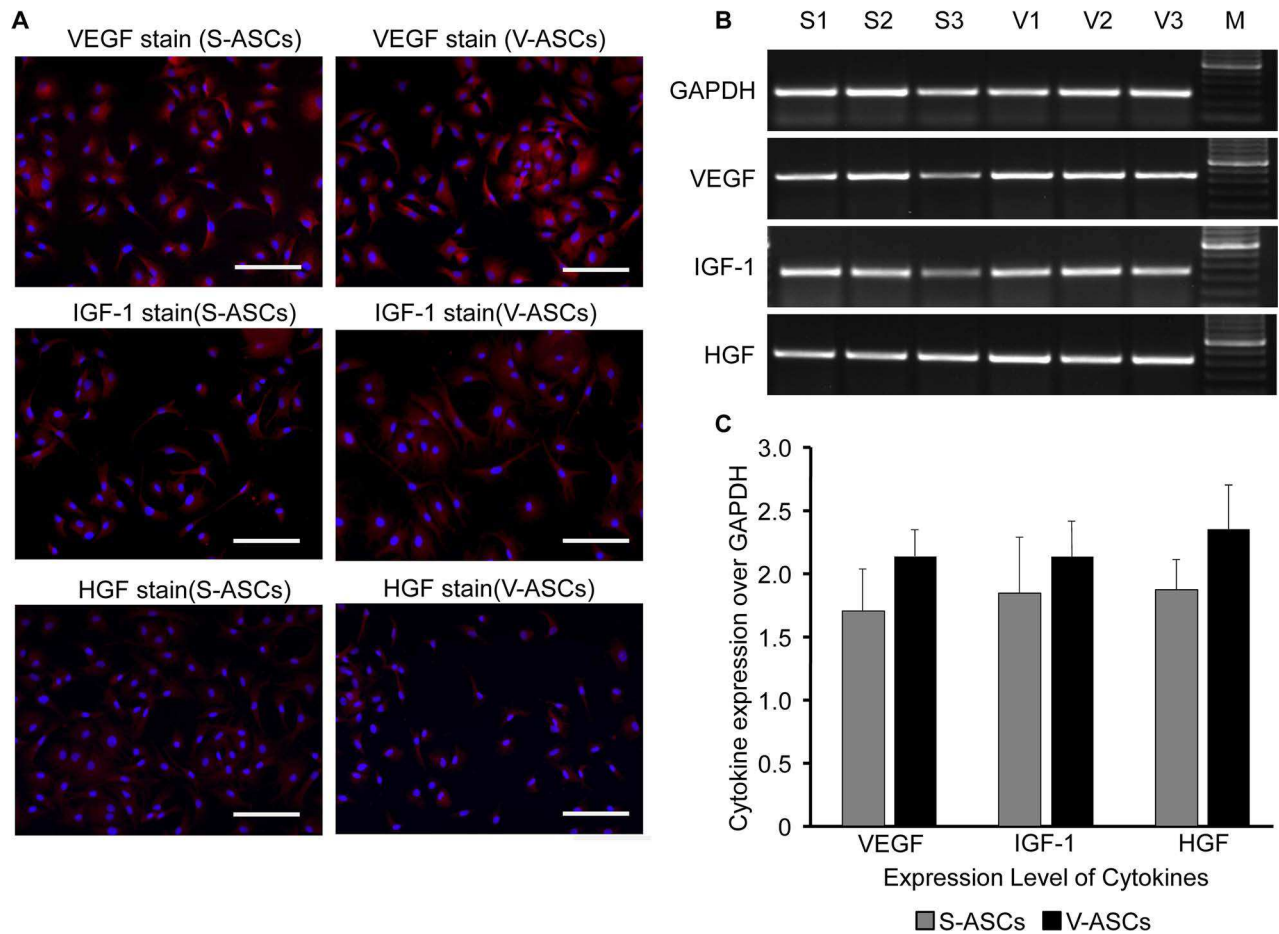


Figure 5. ASC secretions of cell growth factors. Immunofluorescence analysis showed that both S-ASCs and V-ASCs were stained positive with three growth factors (VEGF, IGF-1, and HGF) (A, $n=3$). RT-PCR confirmed mRNA expressions of the three cytokines (B and C, $n=3$). Scale bars: 100 μ m. VEGF, vascular endothelial growth factor; HGF, hepatocyte growth factor; IGF-1, insulin-like growth factor 1.

signal voids in ventricular wall (Fig. 8). Similar voids of MRI signals were not observed on the MR images acquired from the DMEM-treated hearts. Moreover, SPIOs were also found on the tissue sections of the S-/V-ASC-treated rat hearts (Fig. 8). GFP was also identified in the ASC-treated heart sections (Fig. 9), suggesting that some of the implanted ASCs were still alive and retained in the myocardium for at least 6 months.

DISCUSSION

Adipose tissue has recently attracted a great deal of attention in the stem cell research community. This may be attributed to its two major characteristics. First, adipose tissue is abundant in most diabetic and cardiovascular patients. Stem cell therapy is likely needed in the two groups of patients. In addition, thousands of people spend a significant amount of money to remove adipose tissue for medical and cosmetic causes each year, indicating that the harvesting of adipose tissue for collections of

stem cells is likely accepted by the majority of population. Second, the frequency of ASCs in adipose tissue is higher than that of MSCs in bone marrow (7,34). Thus, a sufficient number of stem cells may be acquired from adipose tissue without in vitro expansion. All of these factors suggest that adipose tissue may become an alternative source for MSC collections.

Several studies have shown that transplantation of S-ASCs enhanced mechanical function of infarcted hearts, improved functional recovery of hindlimbs of animals with spinal cord injuries, and increased glucose tolerance in diabetic animals (3,14,19). However, most of the studies focused only on S-ASCs. Therapeutic capacity of ASCs from other adipose deposits, such as visceral deposits, has not been addressed. This study was therefore designed to determine whether V-ASCs could reduce infarct size and improve cardiac function of infarcted hearts. In this study, we found that intramyocardial injections of V-ASCs significantly improved contractile

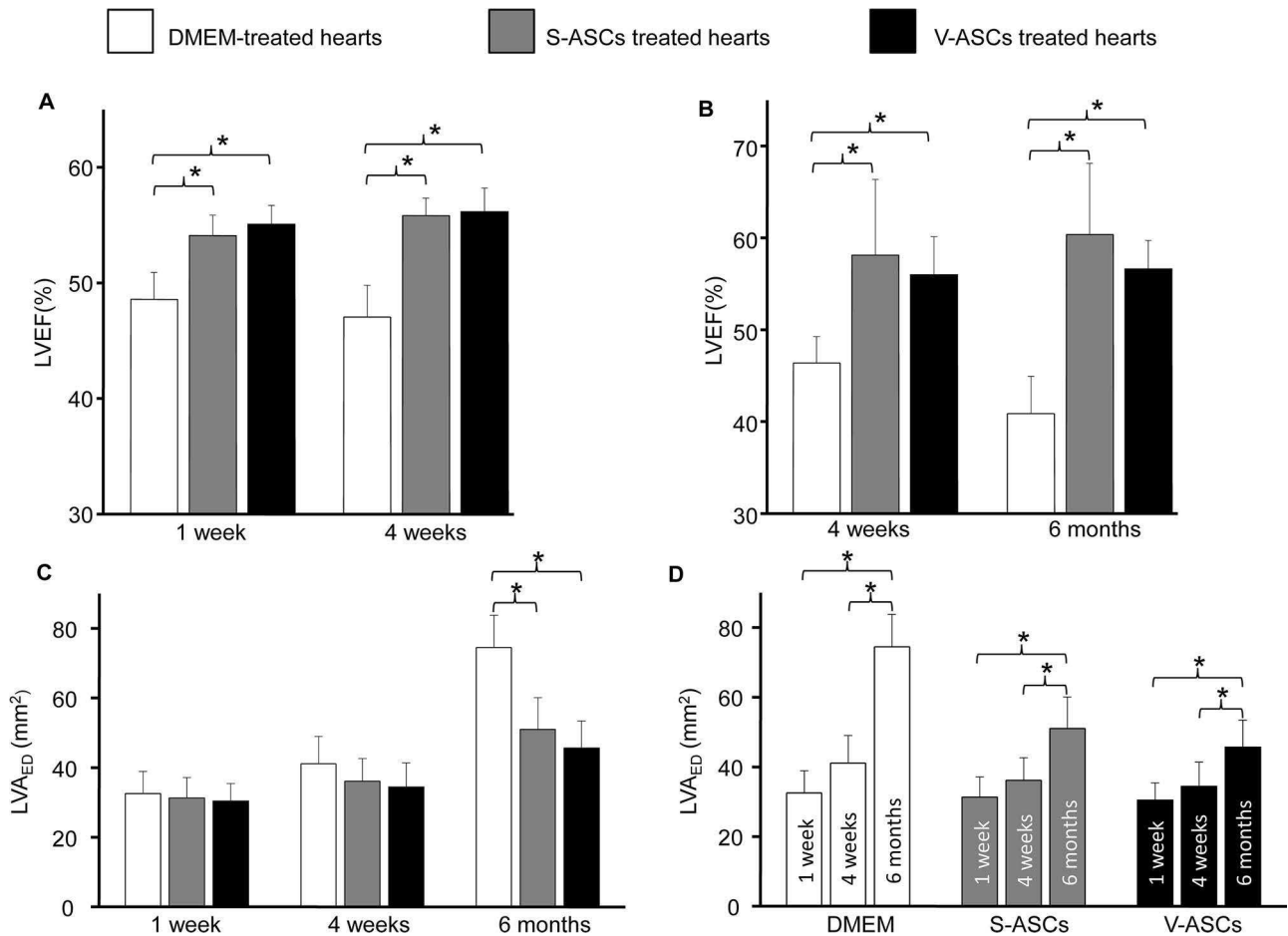


Figure 6. Contractile function of the infarcted rat hearts. The S-ASC-treated ($n=11$) and V-ASC-treated ($n=11$) rat hearts had a significantly ($p < 0.05$) higher left ventricular ejection fraction (LVEF) than the DMEM-treated ($n=10$) hearts at 1 week and 4 weeks after ASC/DMEM transplantations (A). The cardiac functional improvement was also observed in the S-ASC-treated hearts (group IV, $n=11$) and the V-ASC-treated groups (group V, $n=11$) 6 months after the transplantation relative to those treated with DMEM (group VI, $n=10$) (B). The difference in LVEF between the S-ASC- and V-ASC-treated hearts was not statistically significant ($p > 0.05$) at all three points of recovery time. Moreover, the DMEM-treated rat hearts had a significantly ($p < 0.05$) greater LV area at end of diastole (LVA_{ED}) than the S-ASC-treated and V-ASC-treated hearts at 6 months after transplantation (C). At 1 week and 4 weeks following the transplantations, LVA_{ED} was not significantly different among the three groups. LVA_{ED} at 6 months was significantly larger than those measured at 1 week and 4 weeks following the transplantations in all the three groups (D).

function of infarcted rat hearts as did S-ASCs. The cardioprotective benefit lasted for 6 months.

In this study, we first compared cell-surface marker profiles of V-ASCs and S-ASCs. CD29, CD59, CD73, and CD90 were chosen as representative MSC cell-surface markers. As shown in Figure 1, both V-ASCs and S-ASCs exhibited comparable and significant expressions of the CD markers. Moreover, neither V-ASCs nor S-ASCs expressed significant levels of CD11b, CD31, CD45, and CD106. The results suggest that ASCs from the two deposits were similar at the least with respect to cell-surface marker profile.

In addition, it was also noted that V-ASCs had a significantly higher frequency of plastic adherence and colony-forming units per gram of tissue than the S-ASCs, suggesting

that the visceral adipose tissue contains more ASCs than does the subcutaneous adipose tissue. Similarly, Russo and colleagues found that the number of viable stromal vascular fraction (SVF) cells was significantly higher in the human omental adipose tissue than in the human subcutaneous adipose tissue (26). The authors believed that the reason for more SVF cells in the omental than in subcutaneous adipose tissue may be partially related to the greater vascularization in the former than in the latter. However, when the colony-forming unit was expressed as the number of colonies per 100 ASCs, it was found that S-ASCs had a higher colony-forming unit (13.2 colonies/100 S-ASCs) than V-ASCs (9.7 colonies/100 V-ASCs).

As mentioned above, we found that the proliferation rate of S-ASCs and V-ASCs was similar in the first 6 days

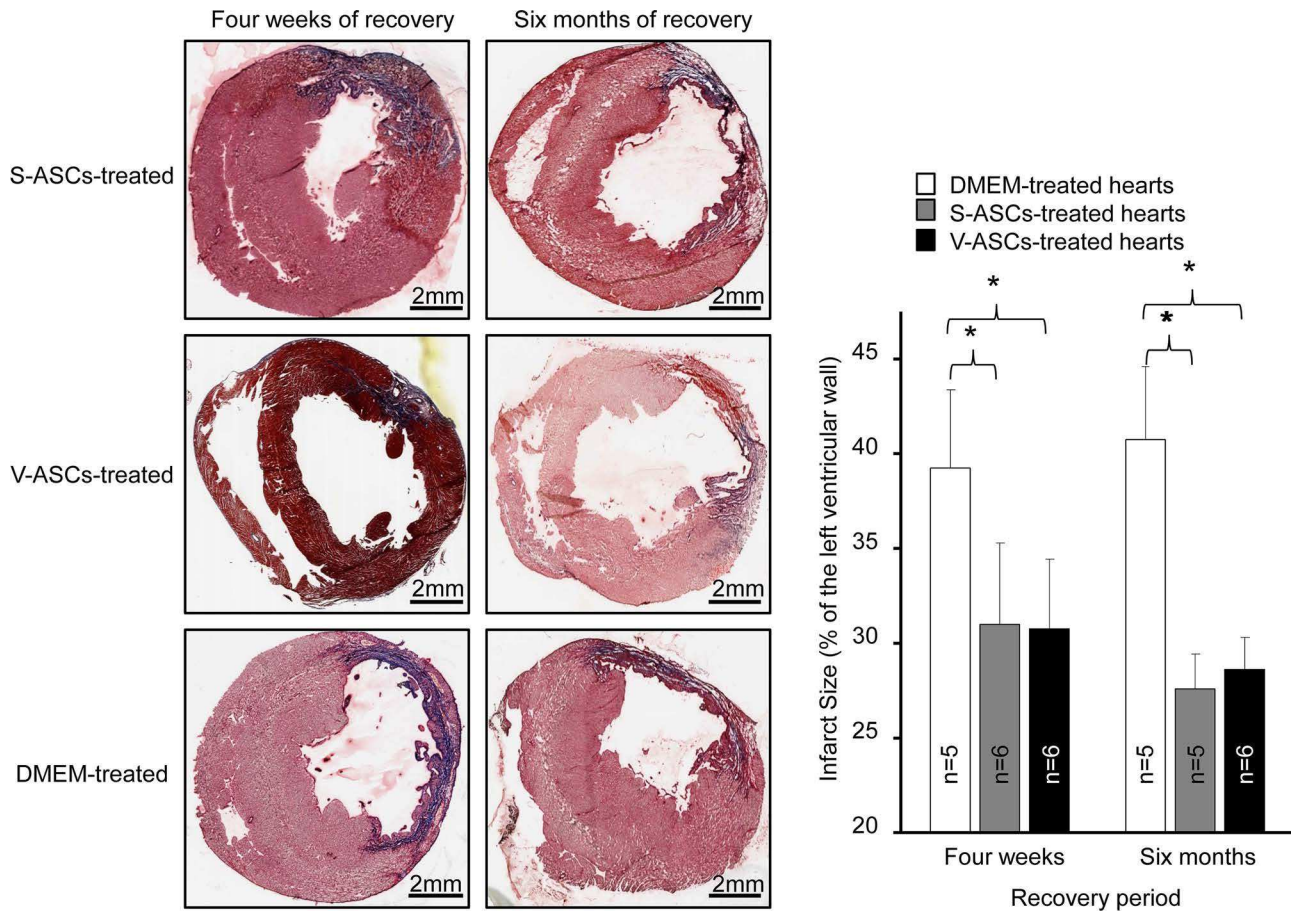


Figure 7. Comparison of infarct size among the S-ASC-treated, V-ASC-treated, and DMEM-treated rat hearts. The S-ASC-treated hearts and V-ASC-treated hearts showed a significantly smaller infarct size than those treated with DMEM. * $p < 0.05$.

of culture. Similar findings were reported by Engel and colleagues (12). In their study, they found that the two types of ASCs proliferated at a comparable rate during 4 days of cultivation. Moreover, we found that the proliferation rate of S-ASCs was significantly higher than that of V-ASCs from the ninth day of culture and on. Baglioni and colleagues reported that human S-ASCs expressed a significantly greater level of BMI-1 (B lymphoma Mo-MLV insertion region 1 homolog) than did V-ASCs (1). BMI-1 has been reported to play a crucial role in self-renewal of stem cells (30). The greater expression of BMI-1 in S-ASCs was the most likely mechanism for the greater CFU and proliferation rate in S-ASCs than in V-ASCs.

Next, we went on to compare differentiation capacity of the V-ASCs and S-ASCs. Adipogenic and osteogenic inductions were conducted at the primary passage of ASCs. As shown in Figure 3, the two sources of ASCs showed a similar percentage (~70%) of Oil red O staining and AP staining following the inductions. Expressions of the adipogenesis-specific markers (LPL and PPAR- γ) and osteogenesis-specific markers (SPP1 and SP7) did not

differ significantly between the V-ASCs and S-ASCs. The results indicate that both V-ASCs and S-ASCs have comparable multidifferentiation potential. Their capacity for cardiomyogenic differentiation is currently under investigation in our lab.

It has been suggested that paracrine action may be one of the major mechanisms underlying the beneficial effects observed with transplantation of adult stem cells (9,20,22). It is well known that VEGF promotes neoangiogenesis, mobilizes stem cells from their niches, and enhances cardiomyocyte proliferation (32,37). HGF is involved in regeneration of various tissues, including myocardium (24). IGF-1 has been shown to enhance cell proliferation and has antiapoptotic function (27). Evidently, expression of the cytokines by implanted stem cells would be helpful in repairing damaged tissues and resuming their normal functions. Therefore, secretion of the three cytokines by both V-ASCs and S-ASCs was assessed using RT-PCR in this study. V-ASCs and S-ASCs were found to secrete similar levels of the cytokines (Fig. 5). Taking the results on cell-surface markers, differentiations, and cytokine

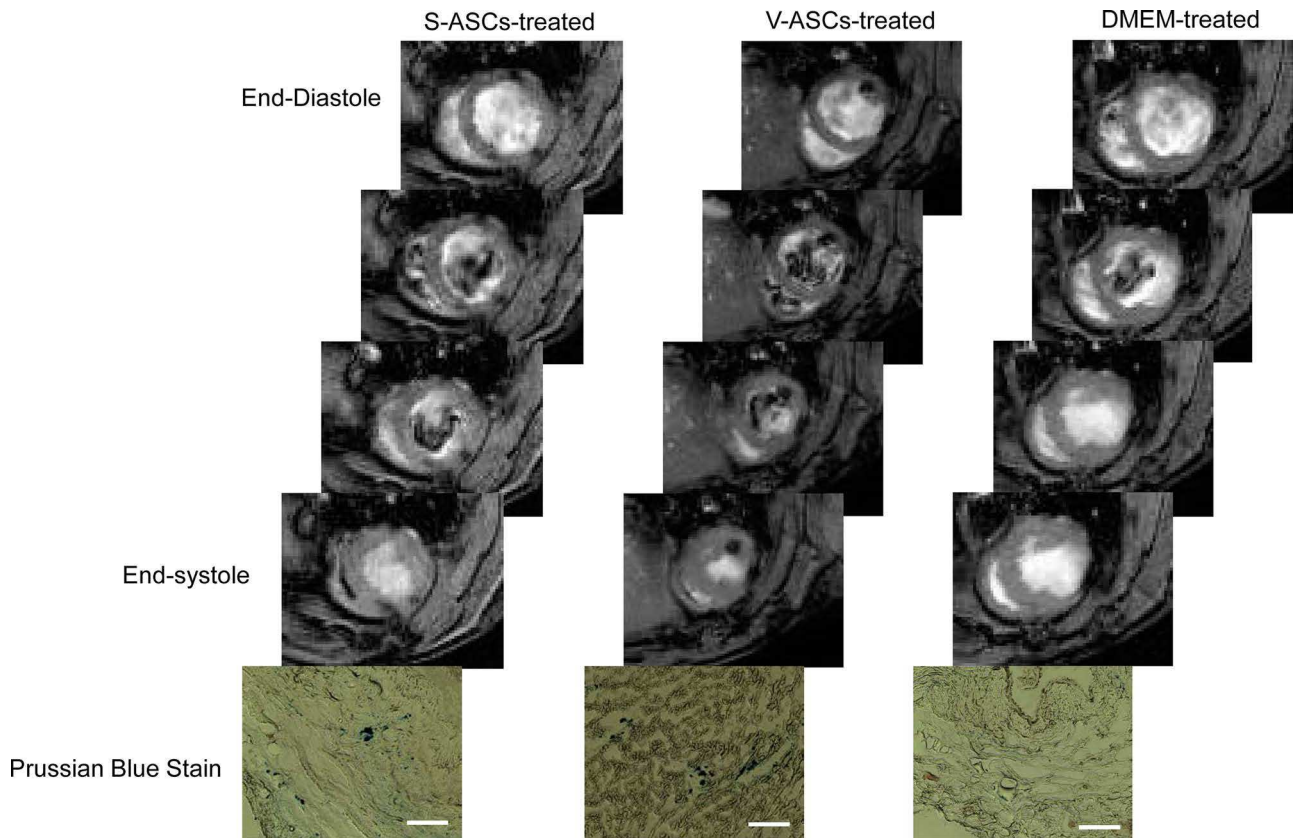


Figure 8. Representative magnetic resonance images and Prussian blue-stained tissue sections of the rat hearts. The S-ASC-treated and V-ASCs-treated rat hearts showed evident MRI signal voids on left ventricular wall at 6 months following ASC injection. On the MR images of the DMEM-treated rat hearts, no similar signal voids were found. The tissue sections of the S-ASC- and V-ASC-treated hearts were stained positive for superparamagnetic iron oxide. Scale bars: 200 μm .

secretion all together, it seems logical to conclude that V-ASCs and S-ASCs are not very different.

The major objective of this study was to determine the cardioprotective effects of the two types of ASCs. To do so, ASCs from the two different sources were injected into the infarct rim of the infarcted rat hearts in respective groups. The cell injections were carried out 1 week after LAD occlusion. This cell transplantation time was chosen to increase survival of the implanted cells. It has been shown that the inflammatory process in response to LAD occlusion is reduced significantly after 1 week (33). Additionally, in our institute, each animal is only allowed to be anesthetized four times throughout a study. Thus, groups I, II, III and groups IV, V, VI were designed to evaluate short- and long-term effects of ASCs, respectively, on cardiac function. It was found that rat hearts treated with either S-ASCs or V-ASCs (S-/V-ASCs) had a significantly greater LVEF than those that received DMEM (Fig. 6). Similar findings were reported by other investigators (5,16,21). In most of the studies, however, animals after cell transplantation were only allowed to recover for 1 to 2 months. Long-term effects of stem cells on cardiac function

were not investigated. In the present study, we followed cardiac function with MRI for 6 months following cell transplantation. The improvement in LVEF observed at 1 week (groups II and III) after cell transplantation indicated that S-ASCs and V-ASCs exerted functional improvement immediately after being delivered to target tissue. Evidently, the enhancement of cardiac function could not be attributed to cardiomyogenic differentiation. The potential mechanism was quite possibly related to paracrine actions of ASCs. As shown in Figure 5, both S-ASCs and V-ASCs secreted significant levels of the proregeneration cytokines. As mentioned above, a couple of studies have shown that stem cell-associated functional improvement was transient and did not last for a significant period of time (8). In contrast, we found that the hearts treated with S-/V-ASCs showed a significantly greater LVEF 6 months after the cell transplantation, indicating that ASCs could improve heart function for a clinically significant period of time. Moreover, the two ASC-treated groups of the rat hearts showed a slight increase in LVEF during 6 months of recovery, whereas in the same period the DMEM-treated rat hearts showed a small decrease in LVEF.

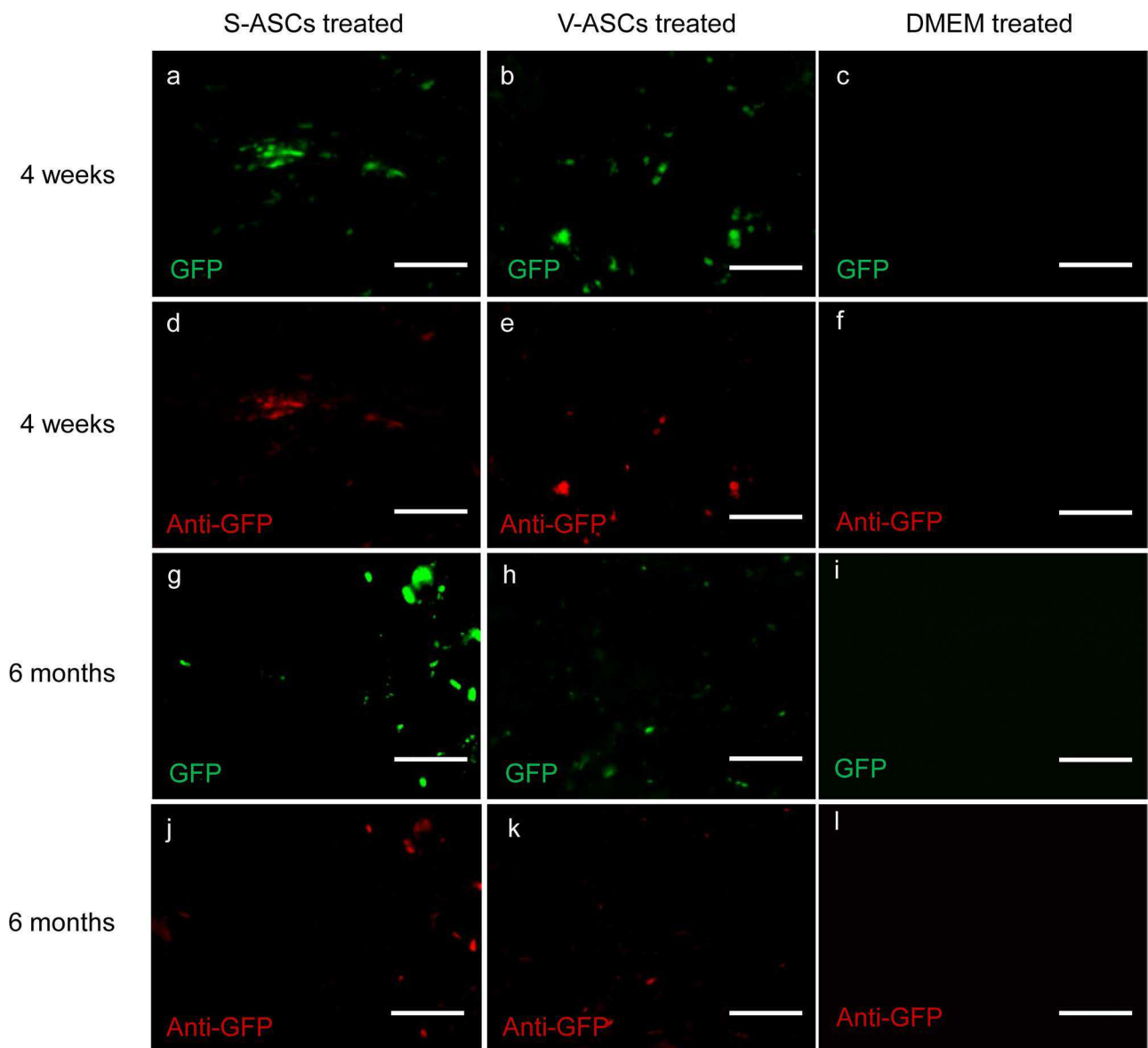


Figure 9. Representative microscopic pictures of the heart sections. Pictures on the first and third rows were acquired with excitation and emission wavelengths set for green fluorescent protein (GFP). Pictures on the second and fourth rows were taken with anti-GFP antibody. Tissue sections from S-ASC- and V-ASC-treated rat hearts showed a few green dots, presumably GFP-labeled ASCs (A, B, G, H). These green dots overlapped with anti-GFP antibody (D, E, J, K), suggesting that some of the S-ASCs and V-ASCs might survive for 6 months following the transplantations. There were no green dots or anti-GFP antibody-stained areas in the DMEM-treated hearts. Scale bars: 50 μ m.

In addition, MR images acquired at 4 weeks and 6 months after cell transplantation displayed clear signal voids in cell injection sites (Fig. 8). These signal voids were not observed on the control animals. In this study, the ASCs were labeled with SPIO prior to injection, and the latter disrupted the homogeneity of the local magnetic field. Thus, the signal voids on the MR images were caused by the SPIO-labeled ASCs. However, the signal voids did not provide information as to the viability of the implanted ASCs. It was possible that implanted ASCs were still alive

with SPIO retained in intracellular compartments. Evidence to support this scenario included GFP dots identified on the heart tissue sections (Fig. 9). However, the frequency of the GFP dots was not very high. Another possible scenario was that the implanted ASCs died and were engulfed by chemotactic macrophages. With staining CD68-positive cells, we did find a few macrophages in the infarct area (data not shown). Furthermore, some of the CD68-positive dots superimposed with the SPIO particles. This suggests that some imported ASCs were dead and engulfed by the

macrophages. Because of the low frequency of the GFP dots, we believe that a great portion of the implanted ASCs migrated to other parts of the body or died shortly after the transplantation. In our previous study (11), the ASCs labeled with ^{18}F -FDG were injected into the rat heart to assess the retention rate of the delivered ASCs. We found that 1 h after transplantation approximately 4.5% and 24% of the ASCs injected into the myocardium remained in the heart and lungs, respectively. Approximately 3.4% and 2.9% of the cells delivered into the myocardium were found in the kidneys and brain. Nevertheless, simultaneous existence of signal voids on MR images and GFP dots on tissue sections indicates their intrinsic correlation. Based on the results, we believe that the validity of MRI for cell tracking holds true for at least 6 months.

As mentioned above, each animal could be only anesthetized four times in our institute. Thus, we could not evaluate heart function prior to the ASC injections. Consequently, self-control comparison was not possible in this study. We believe that self-control analysis is another sensitive approach to assess the effects of implanted stem cells on cardiac function. In addition, only a few animals were included in each of the experimental groups. From a statistical point of view, sample sizes in this study were fairly small. Thus, the validity of the findings in this study needs to be further confirmed.

The present study demonstrates that 1) V-ASCs and S-ASCs share biological properties in cell-surface marker, cytokine secretion, and differentiation capacity; 2) both of them significantly improve cardiac function of infarcted hearts and prevent the deteriorating myocardial remodeling for at least 6 months; and 3) signal voids on MR images reflect existence of viable SPIO-labeled stem cells. In conclusion, ASCs from visceral and subcutaneous fat deposits are equally effective in the treatment of myocardial infarction and heart failure. MRI can be used to follow the implanted stem cells for at least 6 months.

ACKNOWLEDGMENTS: *This research was supported by the Canadian Institutes of Health Research (No. 200806RMF-189873-RMC-CDA4-42533), National Natural Science Foundation of China (No. 81170230 and No. 81200105), and the National Research Council Canada. The authors declare no conflicts of interest.*

REFERENCES

1. Baglioni, S.; Cantini, G.; Poli, G.; Francalanci, M.; Squecco, R.; Di Franco, A.; Borgogni, E.; Frontera, S.; Nesi, G.; Liotta, F.; Lucchese, M.; Perigli, G.; Francini, F.; Forti, G.; Serio, M.; Luconi, M. Functional differences in visceral and subcutaneous fat pads originate from differences in the adipose stem cell. *PloS One* 7(5):e36569; 2012.
2. Baglioni, S.; Francalanci, M.; Squecco, R.; Lombardi, A.; Cantini, G.; Angeli, R.; Gelmini, S.; Guasti, D.; Benvenuti, S.; Annunziato, F.; Bani, D.; Liotta, F.; Francini, F.; Perigli, G.; Serio, M.; Luconi, M. Characterization of human adult stem-cell populations isolated from visceral and subcutaneous adipose tissue. *FASEB J.* 23(10):3494–3505; 2009.
3. Bagno, L. L.; Werneck-de-Castro, J. P.; Oliveira, P. F.; Cunha-Abreu, M. S.; Rocha, N. N.; Kasai-Brunswick, T. H.; Lago, V. M.; Goldenberg, R. C.; Campos-de-Carvalho, A. C. Adipose-derived stromal cell therapy improves cardiac function after coronary occlusion in rats. *Cell Transplant.* 21(9):1985–1996; 2012.
4. Bai, X.; Yan, Y.; Coleman, M.; Wu, G.; Rabinovich, B.; Seidensticker, M.; Alt, E. Tracking long-term survival of intramyocardially delivered human adipose tissue-derived stem cells using bioluminescence imaging. *Mol. Imaging Biol.* 13(4):633–645; 2011.
5. Bai, X.; Yan, Y.; Song, Y. H.; Seidensticker, M.; Rabinovich, B.; Metzeler, R.; Banks, J. A.; Vykoukal, D.; Alt, E. Both cultured and freshly isolated adipose tissue-derived stem cells enhance cardiac function after acute myocardial infarction. *Eur. Heart J.* 31(4):489–501; 2010.
6. Behfar, A.; Crespo-Diaz, R.; Terzic, A.; Gersh, B. J. Cell therapy for cardiac repair--Lessons from clinical trials. *Nat. Rev. Cardiol.* 11(4):232–246; 2014.
7. Constantin, G.; Marconi, S.; Rossi, B.; Angiari, S.; Calderan, L.; Anghileri, E.; Gini, B.; Bach, S. D.; Martinello, M.; Bifari, F.; Galie, M.; Turano, E.; Budui, S.; Sbarbati, A.; Krampera, M.; Bonetti, B. Adipose-derived mesenchymal stem cells ameliorate chronic experimental autoimmune encephalomyelitis. *Stem Cells* 27(10):2624–2635; 2009.
8. Dai, W.; Hale, S. L.; Martin, B. J.; Kuang, J. Q.; Dow, J. S.; Wold, L. E.; Kloner, R. A. Allogeneic mesenchymal stem cell transplantation in postinfarcted rat myocardium: Short- and long-term effects. *Circulation* 112(2):214–223; 2005.
9. Dai, W.; Kay, G. L.; Jyrala, A. J.; Kloner, R. A. Experience from experimental cell transplantation therapy of myocardial infarction: What have we learned? *Cell Transplant.* 22(3):563–568; 2013.
10. De Siena, R.; Balducci, L.; Blasi, A.; Montanaro, M. G.; Saldarelli, M.; Saponaro, V.; Martino, C.; Logrieco, G.; Soleti, A.; Fiobellot, S.; Madeddu, P.; Rossi, G.; Ribatti, D.; Crovace, A.; Cristini, S.; Invernici, G.; Parati, E. A.; Alessandri, G. Omentum-derived stromal cells improve myocardial regeneration in pig post-infarcted heart through a potent paracrine mechanism. *Exp. Cell Res.* 316(11):1804–1815; 2010.
11. Elhami, E.; Dietz, B.; Xiang, B.; Deng, J.; Wang, F.; Chi, C.; Goertzen, A. L.; Mzengeza, S.; Freed, D.; Arora, R. C.; Tian, G. Assessment of three techniques for delivering stem cells to the heart using PET and MR imaging. *EJNMMI Res.* 3(1):72; 2013.
12. Engels, P. E.; Tremp, M.; Kingham, P. J.; di Summa, P. G.; Largo, R. D.; Schaefer, D. J.; Kalbermatten, D. F. Harvest site influences the growth properties of adipose derived stem cells. *Cytotechnology* 65(3):437–445; 2013.
13. Ibrahim, M. M. Subcutaneous and visceral adipose tissue: Structural and functional differences. *Obes. Rev.* 11(1):11–18; 2010.
14. Kang, S. K.; Shin, M. J.; Jung, J. S.; Kim, Y. G.; Kim, C. H. Autologous adipose tissue-derived stromal cells for treatment of spinal cord injury. *Stem Cells Dev.* 15(4):583–594; 2006.
15. Kelley, D. E.; Thaete, F. L.; Troost, F.; Huwe, T.; Goodpaster, B. H. Subdivisions of subcutaneous abdominal adipose tissue and insulin resistance. *Am. J. Physiol. Endocrinol. Metab.* 278(5):E941–948; 2000.

16. Leblanc, A. J.; Nguyen, Q. T.; Touroo, J. S.; Aird, A. L.; Chang, R. C.; Ng, C. K.; Hoying, J. B.; Williams, S. K. Adipose-derived cell construct stabilizes heart function and increases microvascular perfusion in an established infarct. *Stem Cells Transl. Med.* 2(11):896–905; 2013.
17. Lebovitz, H. E.; Banerji, M. A. Point: Visceral adiposity is causally related to insulin resistance. *Diabetes Care* 28(9):2322–2325; 2005.
18. Li, B.; Zeng, Q.; Wang, H.; Shao, S.; Mao, X.; Zhang, F.; Li, S.; Guo, Z. Adipose tissue stromal cells transplantation in rats of acute myocardial infarction. *Coron. Artery Dis.* 18(3):221–227; 2007.
19. Lin, G.; Wang, G.; Liu, G.; Yang, L. J.; Chang, L. J.; Lue, T. F.; Lin, C. S. Treatment of type 1 diabetes with adipose tissue-derived stem cells expressing pancreatic duodenal homeobox 1. *Stem Cells Dev.* 18(10):1399–1406; 2009.
20. Maltais, S.; Tremblay, J. P.; Perrault, L. P.; Ly, H. Q. The paracrine effect: Pivotal mechanism in cell-based cardiac repair. *J. Cardiovasc. Transl. Res.* 3(6):652–662; 2010.
21. Mazo, M.; Hernandez, S.; Gavira, J. J.; Abizanda, G.; Arana, M.; Lopez-Martinez, T.; Moreno, C.; Merino, J.; Martino-Rodriguez, A.; Uixeira, A.; Garcia de Jalon, J. A.; Pastrana, J.; Martinez-Caro, D.; Prosper, F. Treatment of reperfused ischemia with adipose-derived stem cells in a preclinical swine model of myocardial infarction. *Cell Transplant.* 21(12):2723–2733; 2012.
22. Mirosou, M.; Jayawardena, T. M.; Schmeckpeper, J.; Gneccchi, M.; Dzau, V. J. Paracrine mechanisms of stem cell reparative and regenerative actions in the heart. *J. Mol. Cell. Cardiol.* 50(2):280–289; 2011.
23. Naaijken, B. A.; van Dijk, A.; Kamp, O.; Krijnen, P. A.; Niessen, H. W.; Juffermans, L. J. Therapeutic application of adipose derived stem cells in acute myocardial infarction: lessons from animal models. *Stem Cell Rev.* 10(3):389–398; 2014.
24. Nakamura, T.; Mizuno, S.; Matsumoto, K.; Sawa, Y.; Matsuda, H.; Nakamura, T. Myocardial protection from ischemia/reperfusion injury by endogenous and exogenous HGF. *J. Clin. Invest.* 106(12):1511–1519; 2000.
25. Perrini, S.; Ficarella, R.; Picardi, E.; Cignarelli, A.; Barbaro, M.; Nigro, P.; Pescechera, A.; Palumbo, O.; Carella, M.; De Fazio, M.; Natalicchio, A.; Laviola, L.; Pesole, G.; Giorgino, F. Differences in gene expression and cytokine release profiles highlight the heterogeneity of distinct subsets of adipose tissue-derived stem cells in the subcutaneous and visceral adipose tissue in humans. *PLoS One* 8(3):e57892; 2013.
26. Russo, V.; Yu, C.; Belliveau, P.; Hamilton, A.; Flynn, L. E. Comparison of human adipose-derived stem cells isolated from subcutaneous, omental, and intrathoracic adipose tissue depots for regenerative applications. *Stem Cells Transl. Med.* 3(2):206–217; 2014.
27. Sadat, S.; Gehmert, S.; Song, Y. H.; Yen, Y.; Bai, X.; Gaiser, S.; Klein, H.; Alt, E. The cardioprotective effect of mesenchymal stem cells is mediated by IGF-I and VEGF. *Biochem. Biophys. Res. Commun.* 363(3):674–679; 2007.
28. Sanganalath, S. K.; Bolli, R. Cell therapy for heart failure: A comprehensive overview of experimental and clinical studies, current challenges, and future directions. *Circ. Res.* 113(6):810–834; 2013.
29. Seo, M. S.; Jeong, Y. H.; Park, J. R.; Park, S. B.; Rho, K. H.; Kim, H. S.; Yu, K. R.; Lee, S. H.; Jung, J. W.; Lee, Y. S.; Kang, K. S. Isolation and characterization of canine umbilical cord blood-derived mesenchymal stem cells. *J. Vet. Sci.* 10(3):181–187; 2009.
30. Siddique, H. R.; Saleem, M. Role of BMI1, a stem cell factor, in cancer recurrence and chemoresistance: Preclinical and clinical evidences. *Stem Cells* 30(3):372–378; 2012.
31. Strem, B. M.; Zhu, M.; Alfonso, Z.; Daniels, E. J.; Schreiber, R.; Beygui, R.; MacLellan, W. R.; Hedrick, M. H.; Fraser, J. K. Expression of cardiomyocytic markers on adipose tissue-derived cells in a murine model of acute myocardial injury. *Cytotherapy* 7(3):282–291; 2005.
32. Tang, Y. L.; Zhao, Q.; Zhang, Y. C.; Cheng, L.; Liu, M.; Shi, J.; Yang, Y. Z.; Pan, C.; Ge, J.; Phillips, M. I. Autologous mesenchymal stem cell transplantation induce VEGF and neovascularization in ischemic myocardium. *Regul. Pept.* 117(1):3–10; 2004.
33. Vandervelde, S.; van Luyn, M. J.; Rozenbaum, M. H.; Petersen, A. H.; Tio, R. A.; Harmsen, M. C. Stem cell-related cardiac gene expression early after murine myocardial infarction. *Cardiovasc. Res.* 73(4):783–793; 2007.
34. Vidal, M. A.; Kilroy, G. E.; Lopez, M. J.; Johnson, J. R.; Moore, R. M.; Gimble, J. M. Characterization of equine adipose tissue-derived stromal cells: Adipogenic and osteogenic capacity and comparison with bone marrow-derived mesenchymal stromal cells. *Vet. Surg.* 36(7):613–622; 2007.
35. Wang, L.; Deng, J.; Tian, W.; Xiang, B.; Yang, T.; Li, G.; Wang, J.; Gruwel, M.; Kashour, T.; Rendell, J.; Glogowski, M.; Tomanek, B.; Freed, D.; Deslauriers, R.; Arora, R. C.; Tian, G. Adipose-derived stem cells are an effective cell candidate for treatment of heart failure: An MR imaging study of rat hearts. *Am. J. Physiol. Heart Circ. Physiol.* 297(3):H1020–1031; 2009.
36. Zhang, X.; Wang, H.; Ma, X.; Adila, A.; Wang, B.; Liu, F.; Chen, B.; Wang, C.; Ma, Y. Preservation of the cardiac function in infarcted rat hearts by the transplantation of adipose-derived stem cells with injectable fibrin scaffolds. *Exp. Biol. Med.* (Maywood) 235(12):1505–1515; 2010.
37. Zisa, D.; Shabbir, A.; Matri, M.; Suzuki, G.; Lee, T. Intramuscular VEGF repairs the failing heart: Role of host-derived growth factors and mobilization of progenitor cells. *Am. J. Physiol. Regul. Integr. Comp. Physiol.* 297(5):R1503–1515; 2009.
38. Zuk, P. A.; Zhu, M.; Ashjian, P.; De Ugarte, D. A.; Huang, J. I.; Mizuno, H.; Alfonso, Z. C.; Fraser, J. K.; Benhaim, P.; Hedrick, M. H. Human adipose tissue is a source of multipotent stem cells. *Mol. Biol. Cell* 13(12):4279–4295; 2002.